Journal of Hydrology 564 (2018) 501–508

Contents lists available at ScienceDirect

Journal of Hydrology

journal homepage: www.elsevier.com/locate/jhydrol

Research papers

An experimental detrending approach to attributing change of pan evaporation in comparison with the traditional partial differential method

Tingting Wang[a,c], Fubao Sun[a,b,c,e,*], Jun Xia[d,e], Wenbin Liu[a], Yanfang Sang[a], Hong Wang[a]

[a] Key Laboratory of Water Cycle and Related Land Surface Processes, Institute of Geographic Science and Natural Resources Research, Chinese Academy of Sciences, Beijing, China
[b] Ecology Institute of Qilian Mountain, Hexi University, Zhangye City, Gansu Province, China
[c] College of Resources and Environment, University of Chinese Academy of Sciences, Beijing, China
[d] State Key Laboratory of Water Resources and Hydropower Engineering Sciences, Wuhan University, Wuhan 430072, China
[e] Center for Water Resources Research, Chinese Academy of Sciences, Beijing 100101, China

ARTICLE INFO

This manuscript was handled by Tim R. McVicar, Editor-in-Chief, with the assistance of Sergio M. Vicente-Serrano, Associate Editor

Keywords:
Pan evaporation
Attribution
The experimental detrending (ED) approach
The partial differential (PD) method

ABSTRACT

In predicting how droughts and hydrological cycles might change in a changing climate, change of pan evaporation (E_{pan}) is one crucial element to be understood. The derived partial differential (PD) form of the PenPan equation is a prevailing attribution approach worldwide. However, small biases exist and the application of PD method is limited within the derivation of partial differential form of the equation, which impede the attribution analysis in hydrology. Here we designed a series of numerical experiments by detrending each climatic variable, i.e., an experimental detrending (ED) approach, to attribute changes of E_{pan} over China. We compared the attribution results using these two methods and further analyzed the plausible advantages of ED approach. The comparison shows that both ED approach and PD method perform well in attributing changes of E_{pan} and to the input meteorological variables in China over 1960–2017. The first advantage of ED approach is that it can help make robust adjustment for the PD method in attribution analysis. Another advantage lies in its ability to attribute to the observed meteorological variables in China, when the PD method fails to quantify the contribution of relative humidity and air temperature in net radiation in E_{pan} attribution analysis. We highlight that the ED approach is recommended in attribution analysis for hydrologic research. Together with the adjusted PD method, both methods can assist a better understanding and prediction of water-energy cycles change in a changing climate.

1. Introduction

The long-term change of atmospheric evaporative demand, measured using pan evaporation (E_{pan}), is of special concern for understanding how droughts and more generally hydrologic cycle might change in a changing climate. (Brutsaert and Parlange, 1998; Roderick et al., 2007; Zhang et al., 2017). Observed decline in E_{pan} during the past half century, known as the evaporation paradox (Brutsaert and Parlange, 1998; Peterson, 1995), promoted much research interest in attributing changes of E_{pan} worldwide (see comprehensive reviews by Roderick et al. (2009a,b), McVicar et al. (2012) and more recently by Wang et al. (2017)).

In attributing changes of E_{pan}, the correlation/ regression analysis (Nourani and Fard, 2012; Vicente-Serrano et al., 2014) has been used for its simplicity in investigating the relationship between the E_{pan} and meteorological forcings (Li et al., 2014). However, the significant correlation among input meteorological variables would result in considerable biases in attributing changes of E_{pan} using the correlation/ regression approaches. Whilst effective, the correlation methods are not physically based and thus do not reveal causality. Roderick et al. (2007) developed a partial differential (hereafter denoted as PD) form of the PenPan model, to attribute changes of E_{pan} with respect to meteorological variables. The PD method has a simple and physically transparent form and hence has been widely used to quantify the changes of E_{pan}, potential evaporation and etc. (Donohue et al., 2010; Hobbins et al., 2012; Hobbins, 2016; Li et al., 2013; Liu and Sun, 2016, 2017; Roderick et al., 2007; Wang et al., 2015; Wang et al., 2017) This PD method has been applied to some hydrological equations, e.g., the Penman-type potential evaporation equation (Liu and Mcvicar, 2012; Roderick et al., 2007) and the simple Budyko curve (Roderick and

* Corresponding author at: Key Laboratory of Water Cycle and Related Land Surface Processes, Institute of Geographic Science and Natural Resources Research, Chinese Academy of Sciences, China.
E-mail address: Sunfb@igsnrr.ac.cn (F. Sun).

https://doi.org/10.1016/j.jhydrol.2018.07.021
Received 10 August 2017; Received in revised form 3 June 2018; Accepted 11 July 2018
Available online 11 July 2018
0022-1694/

Farquhar, 2011).

However, small biases exist in the attributing results when using the PD method (Roderick et al., 2007; Hobbins et al., 2012; Li et al., 2013; Liu and Sun, 2017), and the application of PD method is limited with clear derivation of partial differential forms of the equations. For more complicated models in hydrology and other fields, for which one could not derive the partial differential forms, a new approach, becomes a helpful alternative. This approach, i.e., the experimental detrending (ED) approach, was developed based on the detrending approach (Hamlet and Lettenmaier, 2007; Mao et al., 2015), has successfully attributed changes of the Palmer Droughts Standard Index (PDSI) to the meteorological variables including precipitation, air temperature, wind speed, sunshine duration and relative humidity (Zhang et al., 2016), which was beyond the ability of PD method in attribution analysis. This indicates that the ED approach can be more widely applied in hydrology research.

In circumstances where both PD method and ED approach can be used in attribution analysis, e.g., attributing changes of E_{pan}, how would ED approach perform in comparison with the widely used PD method? Hence, in this study we aim to design an experiment-based detrending approach to attribute changes of E_{pan} over China using the most recent meteorological observations, and to compare this ED approach with widely applied traditional PD method. Moreover, we are motivated to 1) explore the possible advantages of ED approach and 2) reduce the biases of attribution results when using the traditional PD method in attributing changes of E_{pan}. We present detailed description about both PD method and ED approach along with related data and other method description in Section 2, and the comparison results in Section 3. Followed by discussion in Section 4 and conclusions in Section 5.

2. Data and method

2.1. Data

We collected the most recent daily meteorological data set and the radiation data set provided by the China Meteorological Data Sharing Service System (http://data.cma.cn/) containing 838 stations (maximum) distributed across China. The four major meteorological variables, air temperature (T_a), wind speed at 2 m above ground level (u_2), sunshine duration (Sd) and relative humidity (Rh) cover the period of 1960–2017. The pan (the diameter is 20 cm, hereafter D20) evaporation records are mostly available for the period of 1960–2001, and records in some of the pans are available for 2002–2017. The radiation data set contains 130 sites, and the incoming solar radiation is covering the period of 1960–2014.

Further temporal and spatial consistency control on data was applied based on the information like the length of the time series and spatial distribution of available meteorological data. We chose 416 stations with monthly mean meteorological variables with more than 20 days per month from January 1960 to December 2017 entire time, out of all 838 meteorological stations (see Fig. 1) for the following comparison. For the spatial inhomogeneity problems, we selected grid boxes of 2° × 2° longitude by latitude with at least one selected meteorological station within or very much nearby as mask to avoid the possible interpolation influence (Cai et al, 2010).

2.2. The PenPan model

Rotstayn et al. (2006) coupled the aerodynamic component developed by Thom et al. (1981) with the radiative component of Linacre (1994), and developed a PenPan model based on the mass and energy balance of the pan evaporation. The PenPan model (Eq. (1) can obtain well agreement with measured E_{pan}, and has been well tested around the world (Li et al., 2013; Liu and Sun, 2016; Roderick et al., 2007).

$$E_{pan} = E_{p,R} + E_{p,A} = \left(\frac{\Delta}{\Delta + a\gamma}\frac{R_n}{\lambda}\right) + \left(\frac{a\gamma}{\Delta + a\gamma} f_q(u_2)\cdot(e_s - e_a)\right) \quad (1)$$

where E_{pan} is the pan evaporation rate in kg/(m^2·s) (equivalent to mm/s) and Δ in Pa/K is the slope of the curve created by plotting saturation vapor pressure against air temperature measured at 2 m above the ground; γ (Pa/K) is the psychrometric constant; R_n in W/m^2 is the net available energy (See the detailed calculation in Section S1 in the Supporting information) and λ is the latent heat of vaporization in J/kg; e_s and e_a are the saturate and actual vapor pressure (Pa), respectively. The parameter a (~4.2 for Chinese D20 pan) is the ratio of effective surface area for heat and water-vapor transfer. The commonly used wind function: $f_q(u_2) = 1.39 \times 10^{-8}(1 + 1.35u_2)$ in kg/(m^2·s·Pa) is derived and parameterized by Thom et al. (1981).

However, a large bias exists in the estimated E_{pan} when comparing with observed monthly D20 E_{pan} (Fig. 2a) with Root Mean Square Error (RMSE) of 38.83 mm/month. One possible explanation is that the wind function, which is empirically derived for Class A E_{pan} estimation, is not suitable for D20 E_{pan} estimation, as other parameters or constants are physically based (Rotstayn et al., 2006) in the PenPan model. We used meteorological variables (T_a, Sd, u_2 and Rh) and the corresponding observed D20 E_{pan} in the wind function parameterization. Following Thom's equation, the calibrated wind function is as,

$$f_q(u_2) = 3.977 \times 10^{-8}(1 + 0.505u_2) \quad (2)$$

Improvement has been made with R^2 improving to 0.92 and RMSE decreasing to 26.03 mm/month (Fig. 2b). Hence, the newly adjusted E_{pan} reasonably represents the D20 E_{pan} after using this calibrated wind function, and can thus provide a more accurate basis for attributing changes of E_{pan}.

2.3. The partial differential method

Roderick et al. (2007) developed the PD approach to attribute changes of E_{pan} in Australia. Soon afterwards, it has been widely applied around the world (Hobbins et al., 2012; Li et al., 2013; Liu and Sun, 2016; Prasch and Sonnewald, 2012; Wang et al., 2015) to explain the causes of the declining pan evaporation or potential evaporation. Changes of E_{pan} can be separated to the changes in the radiative component ($E_{p,R}$) and the aerodynamic component ($E_{p,A}$), i.e.,

$$\frac{dE_{pan\_PD}}{dt} = \frac{dE_{p,R}}{dt} + \frac{dE_{p,A}}{dt} \quad (3)$$

To further attribute the changes of E_{pan} to the four key driving variables (R_n, e_a, u_2, and T_a are used here), the detailed decomposition of the first-order $E_{p,R}$ and $E_{p,A}$ expressions are,

$$\frac{dE_{p,R}}{dt} = \frac{\partial E_{p,R}}{\partial R_n}\cdot\frac{dR_n}{dt} + \frac{\partial E_{p,R}}{\partial \Delta}\cdot\frac{d\Delta}{dT_a}\cdot\frac{dT_a}{dt} \quad (4)$$

$$\frac{dE_{p,A}}{dt} = \frac{\partial E_{p,A}}{\partial u_2}\cdot\frac{du_2}{dt} + \frac{\partial E_{p,A}}{\partial e_a}\cdot\frac{de_a}{dt} + \frac{\partial E_{p,A}}{\partial T_a}\cdot\frac{dT_a}{dt} \quad (5)$$

The effect of dT_a/dt on $dE_{p,A}/dt$ can be approximated as the sum of $d\Delta/dT_a \cdot dT_a/dt$ and $de_s/dT_a \cdot dT_a/dt$, in that changes in Δ and e_s can be attributed solely to the changes to T_a. The contribution of T_a in E_{pan} is from both $E_{p,R}$ and $E_{p,A}$, given by,

$$\frac{\partial E_{pan}}{\partial T_a}\cdot\frac{dT_a}{dt} = \frac{\partial E_{p,R}}{\partial \Delta}\cdot\frac{d\Delta}{dT_a}\cdot\frac{dT_a}{dt} + \frac{\partial E_{p,A}}{\partial \Delta}\cdot\frac{d\Delta}{dT_a}\cdot\frac{dT_a}{dt} + \frac{\partial E_{p,A}}{\partial e_s}\cdot\frac{de_s}{dT_a}\cdot\frac{dT_a}{dt} \quad (6)$$

In the above equations, the linear trends (e.g., dT_a/dt in Eqs. (4)–(6) are derived from the meteorological observations, and the sensitivity expressions (e.g., $\partial E_{pan\_PD}/\partial T_a$, in Eq. (6)) are estimated based on the monthly mean of related the meteorological variables. Besides, the model parameters (e.g., a, γ, and λ) can be obtained from previous research (Li et al., 2013; Roderick et al., 2007).

With the derivation above, the attribution results, i.e., dE_{pan_PD}/dt,

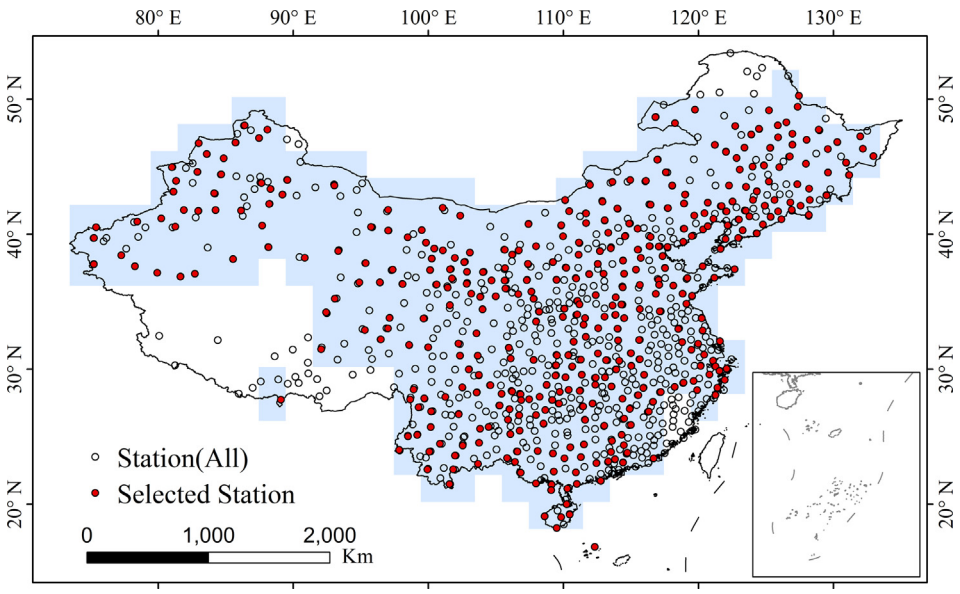

Fig. 1. The study area with all meteorological stations (838 sites) meeting the data control (red dot, 416 sites) and that with mask generated using grid boxes of 2° × 2° longitude by latitude with at least one selected meteorological station within or very much nearby. (For interpretation of the references to color in this figure legend, the reader is referred to the web version of this article.)

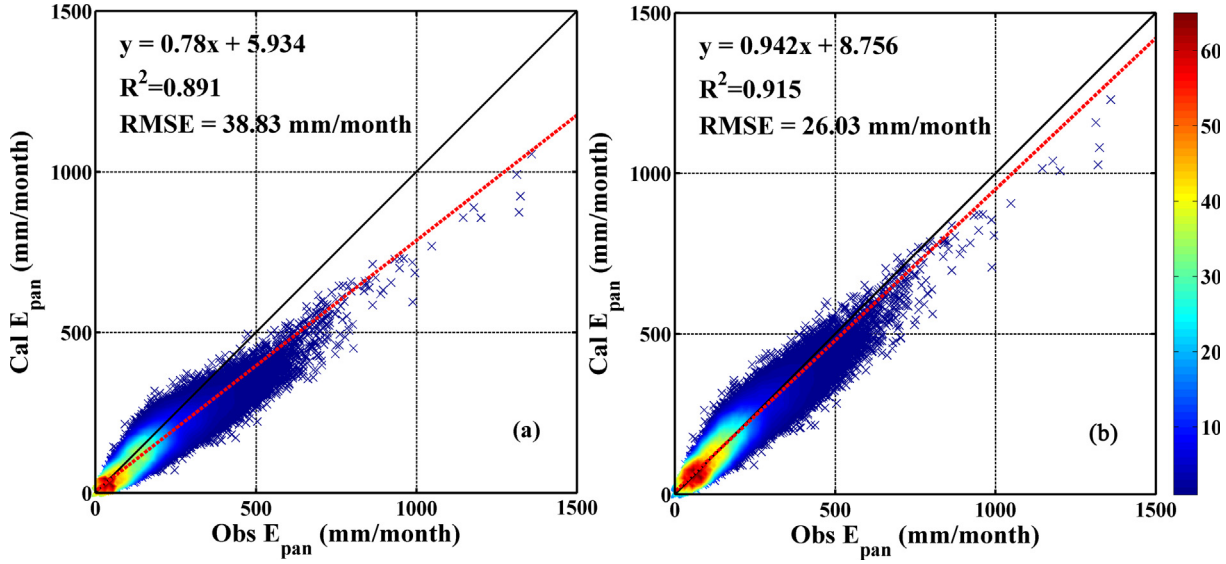

Fig. 2. Comparison between observed and calculated E_{pan} using the wind function derived by Thom et al. in (a) and the calibrated one of $f_q(u_2) = 3.977 \times 10^{-8}(1 + 0.505u_2)$ in (b).

are the sum of contributions of four meteorological variables and can be expressed as,

$$\frac{dE_{pan\_PD}}{dt} \approx \frac{\partial E_{p,R}}{\partial R_n}\cdot\frac{dR_n}{dt} + \frac{\partial E_{pan}}{\partial T_a}\cdot\frac{dT_a}{dt} + \frac{\partial E_{p,A}}{\partial u_2}\cdot\frac{du_2}{dt} + \frac{\partial E_{p,A}}{\partial e_a}\cdot\frac{de_a}{dt} \quad (7)$$

The attribution result dE_{pan_PD}/dt, is then evaluated against the linear trend of observed E_{pan}, i.e., dE_{pan}/dt, at each station.

2.4. The experimental detrending approach

Research on climate change is mainly focused on the trend of meteorological variables and thus their changes in a changing climate. The detrending approach helps eliminate the long-term trends in original meteorological variables so as to separate the roles of climate trend and its variability for a given variable (Hamlet and Lettenmaier, 2007; Lan et al., 2013). Zhang et al. (2016) improved this detrending approach and designed a series of numerical experiments to remove the trends of other independent variables and to retain only a single independent trend, which still preserves the internal relation among the inputs and offers a reasonable separation of attribution results. They have successfully attributed the trend of PDSI to the input variables, which is beyond the ability of PD method. Hence, this method, called the experimental detrending (ED) approach here, can be adopted as an alternative to attribute changes of E_{pan}.

First, we need to generate the newly detrended data sets. We calculated the monthly time series of *Rn* based on *Sd*, *Rh* and T_a, and e_a based on *Rh* and T_a for each station (please see detailed description in Supporting Information), and used *Rn*, T_a, e_a and u_2 as inputs in the following process so that the attribution results are comparable with those using the PD method. The linear trends of T_a, *Rn*, u_2 and e_a, i.e., dT_a/dt, dRn/dt, du_2/dt and de_a/dt, were calculated over 1960–2017 for each given station. The pivotal year (i_{pivot}), 1960, was chosen as the starting years upon which the linear trend was removed from the monthly time series in each station. In detail, the detrended dataset of T_a was as,

$$T_{a\_\,\mathrm{detrend},i,j} = T_{a\_observed,i,j} - k(i - i_{pivot}) \quad (8)$$

where $T_{a\_\mathrm{detrend},i,j}$ is the detrended dataset of T_a in year *i* (1960,

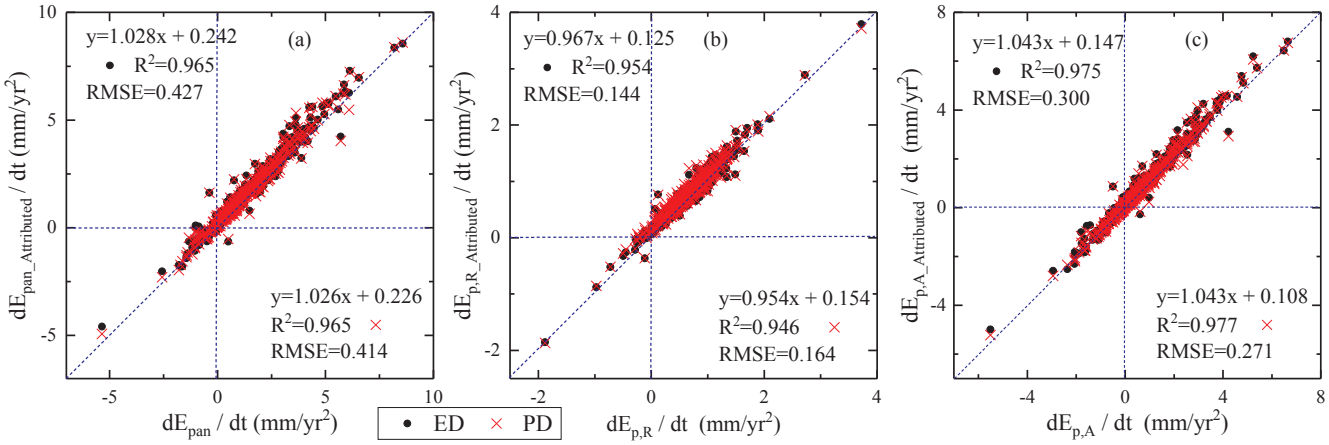

Fig. 3. Comparison of attributed trend of E_{pan} based on the experimental detrending (ED) approach and the traditional partial differential (PD) method ($dE_{pan\_Attributed}/dt$ in y-axis) for 416 selected stations over 1960–2017 in (a). (b) and (c): Same as (a) but for the radiative component ($E_{p,R}$) and aerodynamic component ($E_{p,A}$), respectively. The input variables are *Rn*, T_a, e_a and u_2 for both two attribution methods.

1961, …, 2017) and month *j* (1, 2, …, 12), and $T_{a\_observed,i,j}$ is historical (observed) monthly mean T_a in the same time; *k* is the linear trend of annual T_a at each station.

Since u_2, *Rn* and e_a are generally bounded by 0, the detrending process of these three variables were based on Eqs. (9) and (10),

$$F_{detrend,i,j} = F_{observed,i,j} - k(i - i_{pivot}) \tag{9}$$

$$F_{detrend,i,j} = F_{observed,i,j}\left(\frac{F_{detrend,i}}{F_{observed,i}}\right) \tag{10}$$

where $F_{detrend,i}$ is the detrended annual mean time series of u_2, *Rn* and e_a respectively in year *i*, and $F_{observed,i}$ is historical forcings during the same time. $F_{detrend,i,j}$ is the detrended monthly forcing in year *i* and month *j* and $F_{observed,i,j}$ is the corresponding historical variable.

After the trend in each station was removed from monthly data, the original monthly datasets ($T_{a\_observed,i,j}$ and $F_{observed,i,j}$) were scaled to recreate the detrended monthly datasets while retaining the time series elements of the monthly variations within the year. The inter- and intra-annual variability of the historical climate records are thus preserved since the detrended datasets are constructed through perturbing the historical time series with the linear trends.

Then, we form the annual time series of E_{pan} based on the newly generated detrended data sets. Step one, we calculated the E_{pan} using the detrended monthly meteorological forcings, i.e., $T_{a\_detrend,i,j}$ for T_a and $F_{detrend,i,j}$ for u_2, *Rn* and e_a, to form the base scenario of E_{pan}, and denoted this E_{pan} as $E_{BaseCase}$ for each station. Then the linear trend of $E_{BaseCase}$ (denoted as $dE_{BaseCase}/dt$) represents the trend of E_{pan} without the effect of climate change. Step two, we released the trend of one climatic factor at a time, e.g., for releasing the trend of T_a, we used $T_{a\_observed,i,j}$ for T_a and $F_{detrend,i,j}$ for u_2, *Rn* and e_a to calculate E_{pan} (denoted as $E_{detrend,Ta}$). The trend of $E_{detrend,Ta}$ represents the rate of change of E_{pan} with the warming effect only. We released the trend of T_a, u_2, *Rn* and e_a respectively, and then the corresponding trend of E_{pan} (denoted as $dE_{detrend,f}/dt$, and the subscript *f* is the meteorological forcing of T_a, u_2, *Rn* and e_a respectively) represents the rate of change of E_{pan} with the effect of increasing/decreasing in T_a, u_2, *Rn* and e_a in climate change scenarios respectively. Step three, we got the difference between $dE_{detrend,f}/dt$ and $dE_{BaseCase}/dt$ using Eq. (11). Then this difference can be seen as the contribution of that forcing (C_f) for E_{pan} in each station.

The sum of the contribution of these four meteorological forcings (Eq. (12) in each station is the attributed trend of E_{pan} based on ED approach (denoted as dE_{pan_ED}/dt),

$$C_f = dE_{detrend,f}/dt - dE_{BaseCase}/dt \tag{11}$$

$$\frac{dE_{pan\_ED}}{dt} \approx C_{T_a} + C_{u_2} + C_{Rn} + C_{e_a} \tag{12}$$

Finally, the attribution results (dE_{pan_ED}/dt) were then evaluated against the linear trend of observed E_{pan} (dE_{pan}/dt) in each station.

2.5. The adjustment for the PD method

The $E_{BaseCase}$ plays an important role as control run in ED approach and represents the condition of E_{pan} that free from the impact of climate change. The trend of $E_{BaseCase}$ contains the contribution of some possible factors that are relevant but of minor importance except the effect of four major meteorological forcings (*Rn*, u_2, T_a and e_a). It can lead to some bias when this part of influence on E_{pan} has not been well considered. Here we adopt the $E_{BaseCase}$ from ED approach and make a simple adjustment for the PD method (Eq. (13)) in attributing changes of the E_{pan},

$$dE_{pan\_PD_{Adj}}/dt = dE_{pan\_PD}/dt + dE_{BaseCase}/dt \tag{13}$$

where dE_{pan_PD}/dt and $dE_{pan\_PD_{Adj}}/dt$ are the attributed trends of E_{pan} using the traditional PD and the adjusted PD methods. The $dE_{BaseCase}/dt$ is the trend of base case of E_{pan}, which can be seen as the rate change of E_{pan} due to all other possible factors except the contributions from 4 input meteorological variables.

In addition, RMSE is used to evaluate the performance of attributing changes of E_{pan} based on PD method and ED approach against its observed trend, and *n* is the total amout of years involving in this evaluation.

$$RMSE = \sqrt{\sum_{i=1}^{n}(x_i - y_i)^2/n} \tag{14}$$

3. Results

3.1. Attributing changes of E_{pan}

How does this ED approach perform in attributing change of E_{pan} when compared with the widely used PD method? Here we take the calculated E_{pan} and make comparison of the attributed trends of E_{pan}, $E_{p,R}$ and $E_{p,A}$ (y-axis in Fig. 3) using these two attribution methods against the corresponding observed trends (x-axis in Fig. 3) for 416 sites over 1960–2017.

Overall, both methods are robust in attributing changes of E_{pan}, $E_{p,R}$ and $E_{p,A}$ with dots all very close to 1:1 line (Fig. 3), showing that the ED approach performs well in attributing change of E_{pan} as well as that

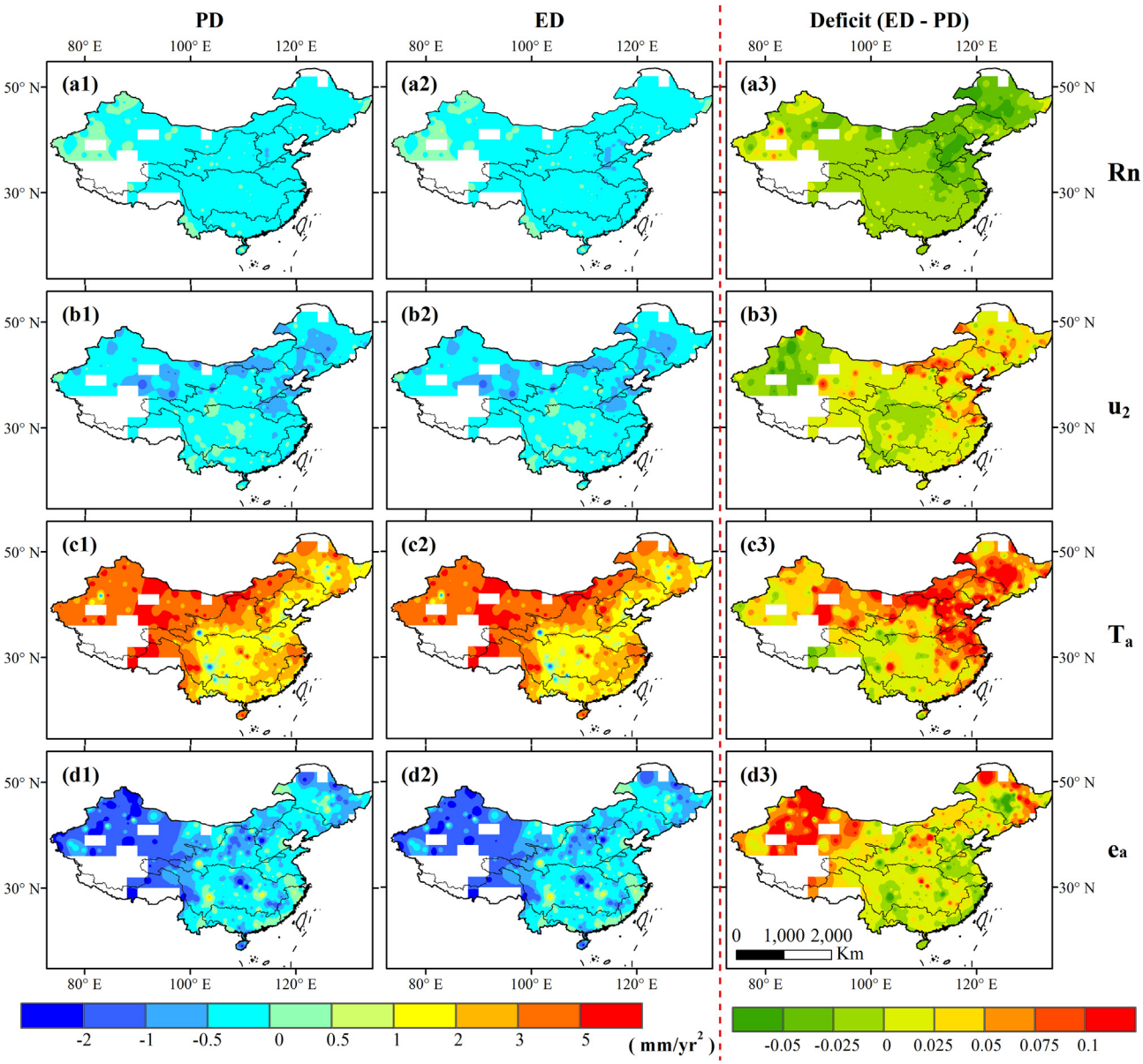

Fig. 4. The spatial distribution of contribution of *Rn*, u_2, T_a and e_a based on PD method (a1–d1, respectively) and ED approach (a2–d2, respectively) using data over 1960–2017, and the color ramp on the left (blue to red) is for the results of two methods. The corresponding deficits (ED - PD) of these variables are in a3–d3 with the color ramp (red to green) on the right. (For interpretation of the references to color in this figure legend, the reader is referred to the web version of this article.)

based on the PD method. Their averages of attributing results for 416 sites are close to the observed linear trends of E_{pan} (dE_{pan}/dt), of $E_{p,A}$ ($dE_{p,R}/dt$) and of $E_{p,R}$ ($dE_{p,A}/dt$) with slopes very approaching to 1.0 and R^2 higher than 0.95. Besides, their RMSE are very similar based on these two attribution methods. To be specific, the RMSE is less than 0.43 mm/yr^2 when attributing change of E_{pan} over the period of 1960–2017, which accounts for a bias of approximately 25% when using these two methods. The biases in $E_{p,A}$ are relatively smaller with RMSE of ~0.30 mm/yr^2 based on ED approach against ~0.27 mm/yr^2 when using PD method. Moreover, the ED approach yields a small improvement in attributing change of $E_{p,R}$ with RMSE of only 0.14 mm/yr^2, which accounts for a bias of less than 20% when compared with that based on the PD method. Above all, the ED approach performs well in attributing change of E_{pan} when compared with the widely used PD method.

3.2. Attributing to meteorological variables

Moreover, the attribution of E_{pan} to the four meteorological variables are compared and presented in Fig. 4. The contribution of *Rn*, u_2, T_a and e_a based on the PD method (Fig. 4a1–d1) and the ED approach (Fig. 4a2–d2) are spatially identical, consistent with the conclusions on attribution of E_{pan} in Section 3.1. While small differences exist in the attribution results between these two methods (Fig. 4a3–4d3). Discrepancy of around 0–0.1 mm/yr^2 is detected for the contribution of T_a, with maximum deficit of 0.94 mm/yr^2 in the northern part of China (Fig. 4b3). Less discrepancies are detected in the contribution of u_2 and e_a with averaged differences of approximately 0.1 mm/yr^2, and also in the contribution of *Rn* with averaged difference of approximately −0.1 mm/yr^2 over the period of 1960–2017. Hence, the ED approach can be used in attributing change of E_{pan} to the input meteorological variables, and their results are very similar to those based on the PD method.

4. Discussion

As mentioned above, one can conclude that the first advantage of ED approach is its wider application in attribution analysis in hydrology with complicated models involved, e.g., attributing changes of PDSI (Zhang et al., 2016), when the usage of PD method is limited within the derivation of partial differential form of the equation, which impede the attribution analysis in hydrology. To explore other possible advantages of this ED approach, we conduct the following analysis.

4.1. Advantage: Better identification and quantification

The change of E_{pan} has been attributed to *Rn*, T_a, e_a and u_2 in the above comparison. However, the e_a is not obtained from observations (estimated based on T_a and *Rh*, please see details in Section S1 in the Supporting information) in China though observed and more commonly used elsewhere around the world. Meanwhile, the observation of *Rn* is rather limited and is often obtained using observations of *Sd*, T_a and *Rh* (Please see details in Section S1 in the Supporting information) instead. Therefore, it can lead to some biases in the total contribution of some variables when attributing change of E_{pan} in each station. Besides, it would offer more information when attributing to the observed meteorological variables. Hence, we try to attribute change of E_{pan} to the observed meteorological variables, i.e., *Sd*, *Rh*, u_2 and T_a for these 416 sites in China.

While using the traditional PD method in the attribution process, it is difficult to decompose the contribution of R_n into the contribution of *Sd*, *Rh* and T_a in that the extraterrestrial radiation (Eq. (4) in Supporting information) is estimated and varied for each day of the year. Hence we use *Rn*, u_2, T_a and *Rh* as inputs and re-attribute change of E_{pan} to these four meteorological variables first, and make comparison of their attribution results using the ED approach (same procedure as Section 2.4 but use *Rh* instead of e_a) and the PD method to present the second advantage of ED approach. The results are shown in Fig. 5a.

Overall, both methods can well attribute changes of Epan to the input variables of *Rn*, u_2, T_a and *Rh*, and the ED approach performs slightly better than the PD method with R^2 a little bit higher (0.94 versus 0.93) and RMSE relatively smaller (0.64 mm/yr^2 versus 0.69 mm/yr^2) for 416 sites over 1960–2017 (Fig. 5a). The discrepancies of the contribution of some variables are relatively small with largest difference of ~0.13 mm/yr^2 in *Rh* and difference of ~0.09 mm/yr^2 in T_a between ED approach and PD methods (Table 1). Moreover, one can concludefrom above comparisons (Sections 3.1 and 4.1) that the ability of these two methods would weaken a little bit with more complicated algorithm involved and the ED approach performs not worse than the PD method.

Furthermore, we use *Sd*, u_2, T_a and *Rh* as input meteorological variables as they are all obtained from observations in China, and conduct the attribution analysis based on the ED approach (denoted as ED2). Then we make comparison of this attribution results against those using *Rn*, u_2, T_a and *Rh* as input meteorological variables (denoted as ED), and the results are shown in Fig. 5b. The ED approach still performs well when using different input variables in attributing change of E_{pan} over 1960–2017 in China (Table 1 and Fig. 5b). The RMSE is 0.638 mm/yr^2, which is very similar to those when attributing to *Rn*, u_2, T_a and *Rh* based on ED approach (RMSE ~0.639 mm/yr^2).

Meanwhile, the contribution of *Rh* in $E_{p,R}$ has been well detected with averaged contribution of -0.05 mm/yr^2 for these 416 sites. Although it is relatively small comparing with other variables, it hits the maximum at 0.39 mm/yr^2 over the period of 1960–2017. Meanwhile, the contribution of T_a in $E_{p,R}$ would be more accurate in that the proportion of the contribution of T_a in Rn (please see details in Section S1 in the Supporting information) has been well quantified when using the ED2 approach. While the proportions of the contribution of *Rh* and T_a are failed to identify and have been overlooked when using the PD method (Table 1) in attributing changes of Epan. Therefore, it can lead to some biases in the total contribution of *Rh* and T_a when attributing change of E_{pan} to the observed meteorological variables using the PD method.

4.2. Advantage: Robust adjustment for the PD method

Based on the calculation process, another advantage of ED approach is the existence of the $E_{BaseCase}$, which indicates the base state of E_{pan} and is directly related to the effect of all other possible factors except the four input meteorological variables. The $E_{BaseCase}$ works as the control run for the attribution analysis when using the ED approach. Then $dE_{BaseCase}/dt$ could be related to the bias of the attribution analysis for the PD method theoretically. Using $E_{BaseCase}$, $E_{BaseCase,R}$ and $E_{BaseCase,A}$, respectively, we adopt Eq. (13) to make adjustment for the PD method in attributing changes of E_{pan}, $E_{p,R}$ and $E_{p,A}$.

Their attribution results using the PD and adjusted PD methods ($dE_{pan\_Attribtued}/dt$, $dE_{p,R\_Attribtued}/dt$, and $dE_{p,A\_Attribtued}/dt$ in y-axis) against the observed linear trend of E_{pan} (dE_{pan}/dt), of $E_{p,R}$ ($dE_{p,R}/dt$), and of $E_{p,A}$ ($dE_{p,A}/dt$) for 416 sites over 1960–2017 are shown in Fig. 6. Clear improvements have been made when using the adjusted PD method with R^2 all higher than 0.99 in three components. Their RMSE are much smaller, reducing from the original 0.41 mm/yr^2 to 0.10 mm/yr^2 for E_{pan}, from 0.16 mm/yr^2 to 0.04 mm/yr^2 for $E_{p,R}$, and from 0.27 mm/yr^2 to 0.09 mm/yr^2 for $E_{p,A}$ for 416 sites. Hence, the adjusted PD method turns out to be effective and can help to improve the attribution results of E_{pan}.

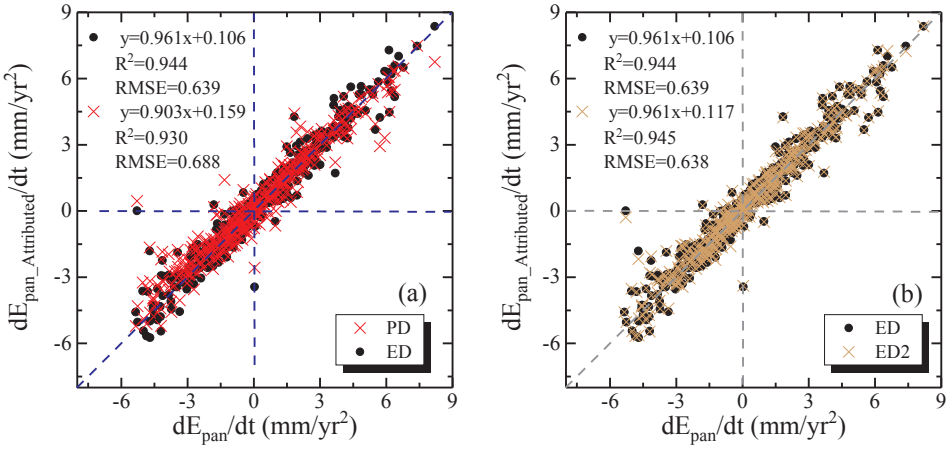

Fig. 5. Comparison of attribution results against the observed rate of change of E_{pan} for 416 sites over the period of 1960–2017. The input variables are *Rn*, T_a, *Rh* and u_2 in (a) when using the PD method and ED approach, and ED2 in (b) means the attribution result using *Sd*, T_a, *Rh* and u_2 as inputs using the ED approach.

Table 1
The averaged change of contribution of u_2, T_a, *Rh and Rn(Sd)* in E_{pan}, $E_{p,R}$ and $E_{p,A}$ in 416 sites for 1960–2017 using ED approach and PD method. The contribution of *Rn* is obtained from both ED approach (ED) and PD method, and the contribution of *Sd* is derived from ED approach (ED2), respectively, unit: mm/yr^2.

	PD			ED			ED2		
	E_{pan}	$E_{p,R}$	$E_{p,A}$	E_{pan}	$E_{p,R}$	$E_{p,A}$	E_{pan}	$E_{p,R}$	$E_{p,A}$
u_2	−2.04		−2.04	−2.12		−2.12	−2.12		−2.12
T_a	1.97	0.75	1.22	2.06	0.76	1.29	2.24	0.94	1.29
Rh	0.92		0.92	0.79		0.79	0.74	-0.05	0.79
Rn (Sd)	−0.64	−0.64		−0.68	−0.68		−0.67	−0.67	

Moreover, we can gain a better understanding of the rate of change of E_{pan}. The effect of four input meteorological variables (R_n, e_a, u_2, and T_a) accounts for ~91% of the total rate of change of E_{pan}. While the rest ~9% due to other possible factors though minor but relevant, is unidentifiable using the traditional PD method but can be well identified and remedied by the adjusted PD method in attributing changes of E_{pan}. An accurate estimation and usage of $E_{BaseCase}$ is crucial for the ED approach and the PD method adjustment. Hence, the third advantage of ED approach is that it can make robust adjustment for PD method and can help gain an in-depth analysis of changes of E_{pan}, and further provide a better way in understanding and prediction of water-energy change in a changing climate.

5. Conclusion

An accurate attribution analysis of E_{pan} is crucial and necessary to understand the evaporative demand and its changes in a changing climate. The prevailing attribution approach, partial differential (PD) method, is usually applied to simple equations with a small bias in the attribution results. Hence we designed a series of numerical experiments by detrending each climatic variable, i.e., an experimental detrending (ED) approach, to provide another attribution approach and to make up that disadvantage of the PD method so as to better attribute change of E_{pan}.

First, clear improvement can be made when using the newly calibrated wind function ($f_q(u_2) = 3.977 \times 10^{-8}(1 + 0.505u_2)$) in the PenPan model in Chinese D20 E_{pan} estimation. Then the comparison of attribution results show that both ED approach and PD method perform well in attributing change of E_{pan} when using R_n, e_a, u_2, and T_a as input meteorological variables. The first advantage of ED approach is its wider application in hydrology with complicated models involved. he second advantage lies in its ability to attribute changes of E_{pan} to *Sd*, u_2,T_a and *Rh*,which are meteorological observations in China. The ED approach can well identify and quantify the contribution of *Rh* and T_a in *Rn*, which have been overlooked when using the PD method. The third advantage is the $E_{BaseCase}$ in ED approach, which works as control run, can make robust adjustment for the traditional PD method. The adjusted PD method turns out to be effective and provides a better understanding of the change of E_{pan}: the contribution of four meteorological variables takes up ~91% of the total rate of change of E_{pan} and can be well identified by the PD method, leaving the rest ~9% due to other possible factors unidentifiable but can be well identified and remedied by the adjusted PD method.

Hence, the ED approach is recommended for its superiority in cases when PD method is capable in attribution analysis as well as in cases with complicated hydrological models involved when the usage of PD method is limited within the derivation of partial differential form of the equation, e.g., attributing of PDSI. Besides, the ED approach can make robust adjustment for the PD method. Therefore, both the ED approach and the adjusted PD method are recommended in attribution analysis in hydrology and hydrometeorology to gain a better understanding and prediction of water-energy changes in a changing climate.

Acknowledgements

This research was supported by the National Key Research and Development Program of China (2016YFC0401401 and 2016YFA0602402), the Key Programs of the Chinese Academy of Sciences (ZDRW-ZS-2017-3-1), the CAS Pioneer Hundred Talents Program (Fubao Sun), an Open Research Fund of State Key Laboratory of Desert and Oasis Ecology in Xinjiang Institute of Ecology and Geography, Chinese Academy of Sciences (CAS). The authors gratefully acknowledge the China Meteorological Data sharing Service System Administration (http://data.cma.cn/) for the data served here. We also wish to thank the editor Tim R. McVicar and associate editor: Sergio M. Vicente-Serrano, and three anonymous reviewers for their invaluable comments and constructive suggestions to improve this manuscript.

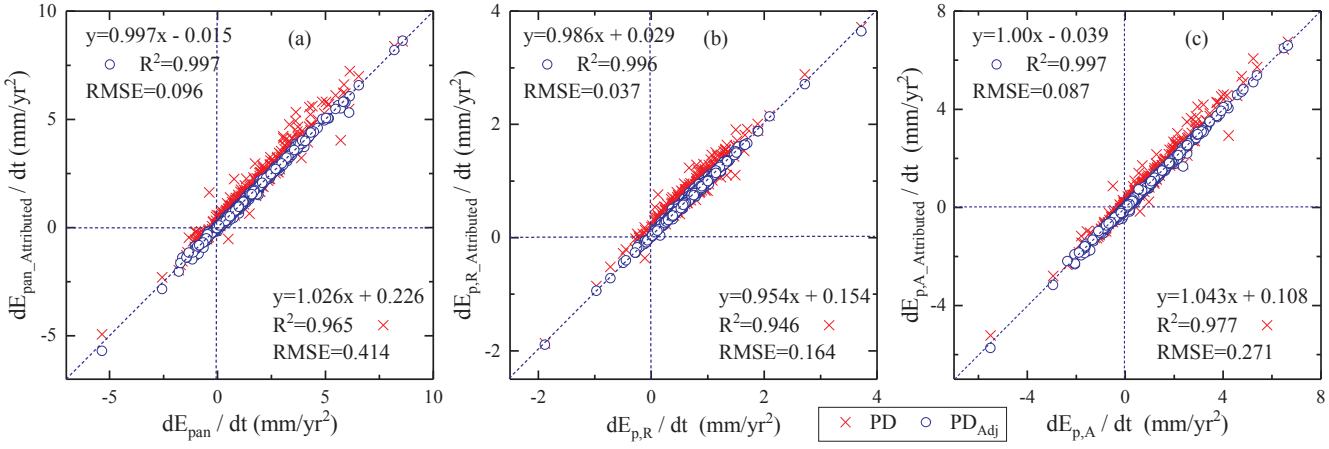

Fig. 6. (a) The comparison of attributed trends of E_{pan} (a), $E_{p,R}$ (b) and $E_{p,A}$ (c) based on PD and adjusted PD methods (y-axis) against their linear trends, i.e., dE_{pant}/dt, $E_{p,R}$/dt and $E_{p,A}$/dt (x-axis) for 1960–2017.

Appendix A. Supplementary data

Supplementary data associated with this article can be found, in the online version, at https://doi.org/10.1016/j.jhydrol.2018.07.021.

References

Brutsaert, W., Parlange, M., 1998. Hydrologic cycle explains the evaporation paradox. Nature 396 (6706) 30 30.

Cai, W., Cowan, T., Braganza, K., Jones, D., Risbey, J., 2010. Comment on "On the recent warming in the Murray-Darling Basin: Land surface interactions misunderstood" by Lockart et al. Geophys. Res. Lett. 37 (10) L10706.

Donohue, R., Roderick, M., McVicar, T.R., 2010. Can dynamic vegetation information improve the accuracy of Budyko's hydrological model? J. Hydrol. 390 (1), 23–34. https://doi.org/10.1016/j.jhydrol.2010.06.025.

Hamlet, A.F., Lettenmaier, D.P., 2007. Effects of 20th century warming and climate variability on flood risk in the western US. Water. Resour. Res. 43 (6), W06427. https://doi.org/10.1029/2006WR005099.

Hobbins, M., Wood, A., Streubel, D., Werner, K., 2012. What drives the variability of evaporative demand across the conterminous United States? J. Hydrometeorol. 13 (4), 1195–1214.

Hobbins, M.T., 2016. The variability of ASCE Standardized reference evapotranspiration: a rigorous. CONUS-wide Decompos. Attrib.

Lan, C., Zhang, Y., Gao, Y., Hao, Z., Cairang, L., 2013. The impacts of climate change and land cover/use transition on the hydrology in the upper Yellow River Basin, China. J. Hydrol. 502, 37–52.

Li, Z., Chen, Y., Shen, Y., Liu, Y., Zhang, S., 2013. Analysis of changing pan evaporation in the arid region of Northwest China. Water. Resour. Res. 49 (4), 2205–2212.

Li, Z., Chen, Y., Yang, J., Wang, Y., 2014. Potential evapotranspiration and its attribution over the past 50 years in the arid region of Northwest China. Hydrological Process. 28 (3), 1025–1031.

Linacre, E.T., 1994. Estimating U.S. Class a pan evaporation from few climate data. Water Int. 19 (1), 5–14.

Liu, Q., Mcvicar, T.R., 2012. Assessing climate change induced modification of Penman potential evaporation and runoff sensitivity in a large water-limited basin. J. Hydrol. s464–465 (20), 352–362.

Liu, W., Sun, F., 2016. Assessing estimates of evaporative demand in climate models using observed pan evaporation over China. J. Geophys. Res.: Atmos. 121 (14), 8329–8349.

Liu, W., Sun, F., 2017. Projecting and attributing future changes of evaporative demand over China in CMIP5 climate models. J. Hydrometeorol. 18 (4), 977–991. https://doi.org/10.1175/jhm-d-16-0204.1.

Mao, Y., Nijssen, B., Lettenmaier, D.P., 2015. Is climate change implicated in the 2013–2014 California drought? A hydrologic perspective. Geophys. Res. Lett. 42 (8), 2805–2813.

McVicar, T.R., et al., 2012. Global review and synthesis of trends in observed terrestrial near-surface wind speeds: implications for evaporation. J. Hydrol. 416, 182–205.

Nourani, V., Fard, M.S., 2012. Sensitivity analysis of the artificial neural network outputs in simulation of the evaporation process at different climatologic regimes. Adv. Eng. Software 47 (1), 127–146.

Peterson, T., 1995. Evaporation losing its strength. Nature 377, 687–688.

Prasch, C.M., Sonnewald, U., 2012. Estimating actual, potential, reference crop and pan evaporation using standard meteorological data: a pramatic synthesis. Hydrol. Earth Syst. Sci. Discuss. 9 (10), 11829–11910.

Roderick, M.L., Farquhar, G.D., 2011. A simple framework for relating variations in runoff to variations in climatic conditions and catchment properties. Water. Resour. Res. 47 (12), W00G07. https://doi.org/10.1029/2010WR009826.

Roderick, M.L., Hobbins, M.T., Farquhar, G.D., 2009a. Pan evaporation trends and the terrestrial water balance. I. Principles and Observations. Geogr. Compass 3 (2), 746–760.

Roderick, M.L., Hobbins, M.T., Farquhar, G.D., 2009b. Pan evaporation trends and the terrestrial water balance. II. Energy balance and interpretation. Geogr. Compass 3 (2), 761–780.

Roderick, M.L., Rotstayn, L.D., Farquhar, G.D., Hobbins, M.T., 2007. On the attribution of changing pan evaporation. Geophys. Res. Lett. 34 (17), 251–270.

Rotstayn, L.D., Roderick, M.L., Farquhar, G.D., 2006. A simple pan-evaporation model for analysis of climate simulations: evaluation over Australia. Geophys. Res. Lett. 33 (17), 254–269.

Thom, A., Thony, J.L., Vauclin, M., 1981. On the proper employment of evaporation pans and atmometers in estimating potential transpiration. Q J. Roy. Meteor. Soc. 107 (453), 711–736.

Vicente-Serrano, S.M., et al., 2014. Sensitivity of reference evapotranspiration to changes in meteorological parameters in Spain (1961–2011). Water. Resour. Res. 50 (11), 8458–8480.

Wang, J., et al., 2015. Temporal and spatial characteristics of pan evaporation trends and their attribution to meteorological drivers in the Three-River Source Region, China. J. Geophys. Res. Atmos. 120, 6391–6408.

Wang, T., Zhang, J., Sun, F., Liu, W., 2017. Pan evaporation paradox and evaporative demand from the past to the future over China: a review. Wiley Interdisciplinary Rev. Water 4 (3). https://doi.org/10.1002/wat2.1207.

Zhang, J., et al., 2016. Dependence of trends in and sensitivity of drought over China (1961–2013) on potential evaporation model. Geophys. Res. Lett. 43 (1), 206–1203.

Zhang, Q., Kong, D., Singh, V.P., Shi, P., 2017. Response of vegetation to different time-scales drought across China: spatiotemporal patterns, causes and implications. Global Planet. Change 152, 1–11.